

Electronic Supplementary Information for:

Orientations of Polyoxometalate Anions on Gold Nanoparticles

Shelly Sharet, Ella Sandars, Yifeng Wang, Offer Zeiri, Alevtina Neyman, Louisa Meshi and Ira A Weinstock*

Table of contents

1. Materials and methods

1.1 Materials

1.2 Syntheses of POM salts containing different counter cations

1.3 Instruments

1.4 Synthesis of citrate-stabilized Au NPs

1.5 POM monolayers formation

1.6 Cryogenic Sample Preparation for Transmission Electron Spectroscopy (Cryo-TEM)

1.7 Measurement of monolayers

Figure S1. Dimensions associated with the monolayer width.

Figure S2. Measurement method used to determine the core and monolayer sizes.

2. Size distribution of the Au NPs

Figure S3. Size distribution of the citrate-stabilized 6 nm Au NPs.

3. Electron density distribution in the Preyssler ion

Figure S4. Top (A) and side (B, one-half of the molecule) views of the molecular electrostatic potential (MEP) distribution for $[\text{NaP}_5\text{W}_{30}\text{O}_{110}]^{14-}$.

4. References

1. Materials and methods

1.1 Materials

The polyoxometalate (POM) salts, α -K₉AlW₁₁O₃₉·13H₂O (K₉1),¹⁻³ and K_{12.5}Na_{1.5}[NaP₅W₃₀O₁₁₀·15H₂O]⁴ (K_{12.5}Na_{1.5}2), Na₁₆[Zn₄(H₂O)₂(P₂W₁₅O₅₆)₂]⁵, (3), and were prepared using the published method. Citric acid, C₆H₈O₇ (AG) was purchased from Frutarom LTD. The cesium salt, Cs₃Ct·~4H₂O was prepared by neutralizing citric acid solutions using hydroxides of the corresponding cations, monitored using a pH meter, and evaporated to dryness. The purities of the POM and citrate salts were checked (as appropriate) by FTIR, cyclic voltammetry (CV), and by ²⁷Al and ³¹P NMR spectroscopy.³ All solutions were prepared using high-purity Millipore[®] water (17 ± 1 MΩ) and all glassware used for synthesis and storage of gold nanoparticles was pre-treated with fresh aqua regia (3:1 v:v ratio of HCl to HNO₃).

1.2 Syntheses of POM salts containing different counter cations

The acid form of the Preyssler anion, H₁₄[NaP₅W₃₀O₁₁₀·58H₂O], was prepared by cation exchange. For that, a ca. 2 mM solution was passed very slowly (approx. 4 mL h⁻¹) through a 60-cm length, 2-cm diameter column packed with ca. 160 mL of Amberlite 200 resin, acid form. The eluent solution was evaporated to dryness under reduced pressure. The amount of residual K⁺ ion was < 0.03% (sodium tetraphenylborate test⁹). The structural integrity was confirmed by ³¹P NMR spectroscopy.

The Li⁺, Na⁺, K⁺, TMA⁺ and Cs⁺ salts of 3 were synthesized by neutralization of H₁₄[NaP₅W₃₀O₁₁₀·58H₂O] by the hydroxides of the corresponding cations, followed by evaporation to dryness by rotary evaporation.

1.3 Instruments

UV-visible spectra were obtained using a Hewlett-Packard 8453 spectrophotometer. Cryogenic sample preparation for transmission electron spectroscopy (cryo-TEM), and image acquisition, were as previously described.⁶⁻⁸ TEM and cryo-TEM images were captured on a FEI Tecnai 12 G² instrument (120 kV) using a Gatan slow-scan camera.

1.4 Synthesis of citrate-stabilized Au NPs

Citrate-stabilized Au NPs colloidal solution was synthesized using the published method with minor modification.⁹ First, 50 ml 0.5 mM HAuCl₄ was stirred for 30 min in an ice bath. Then 158 μL of 0.4 mM cesium-citrate solution was added. The concentration of citrate was ca. 1.3 mM. To this solution, ice-cold fresh NaBH₄ (0.1 M, 50 μL) was added quickly with vigorous stirring and the solution turned deep red immediately. The final solution was stirred for another 50 minutes and stored at 2 °C in refrigerator before use. The pH of the Au NP solution was ca. 5.9. The size distribution was determined by measuring the diameter of ca. 160 nanoparticles in TEM images. The average diameter is 6.4 nm with a standard deviation of 1.4 nm.

1.5 POM monolayer formation.

Thermodynamics for POM-monolayer formation was measured using the previous method.⁷ Based on the thermodynamic data, concentration of each POM sufficient for monolayer formation was determined. The POMs were then reacted with Au NPs. The mixtures were stored in the dark for ca. 24 h before further characterization.

For the reaction of α -K₉AlW₁₁O₃₉ with potassium-citrate stabilized Au NPs, 2 mM of the POM was reacted with an equal volume of cesium-citrate stabilized Au NPs. For the preyssler ion, Cs₁₄[NaP₅W₃₀O₁₁₀·15H₂O], a final concentration of 0.05 mM was used. For the Finke-Droege POM, Na₁₆[Zn₄(H₂O)₂(P₂W₁₅O₅₆)₂], a solid sample which gives 0.05 mM final concentration was added to cesium-citrate stabilized Au NP solution (which contains 6 mM Cs⁺). After equilibration, undissolved POM salt was removed by filtration through a 0.45 μm membrane.

1.6 Cryogenic Sample Preparation for Transmission Electron Spectroscopy (Cryo-TEM).

Cryogenically frozen samples were prepared using a fully automated vitrification device (Leica, EM GP). First, 4 μL of the sample solution was placed by pipet onto a glow discharged Cu grid covered with a lacey-carbon film, held inside a 100%-humidity chamber. Typically, the grid was mechanically “blotted” for 2.5 seconds, and immediately plunged into liquid ethane (mp 90.34 K) cooled by liquid nitrogen (77.2 K). Samples of $\text{AlW}_{11}\text{O}_{39}^{9-}$ -protected Au NPs were also prepared with different blotting times (set at 3, 4 and 5 seconds) followed by variable holding times before plunging, to ensure that variable times to allow for “relaxation” during sampling did not affect the results.

1.7 Measurement of monolayers

General approach. The measurement of lengths was performed using the *DigitalMicrograph* software. The diameter of the core-shell structure, d_{shell} , and the diameter of the Au core, d_{core} , shown in Figure S1, were both measured using the method and criteria discussed below, in connection to Figure S2, and the monolayer width was then calculated as the difference in (eq S1). For each particle, many values of thickness of varying directions are obtained. These values are averaged to give the thickness of the monolayer on this nanoparticle. Statistics on the monolayer thicknesses of many Au NPs (typically > 30) give the reported values in the text.

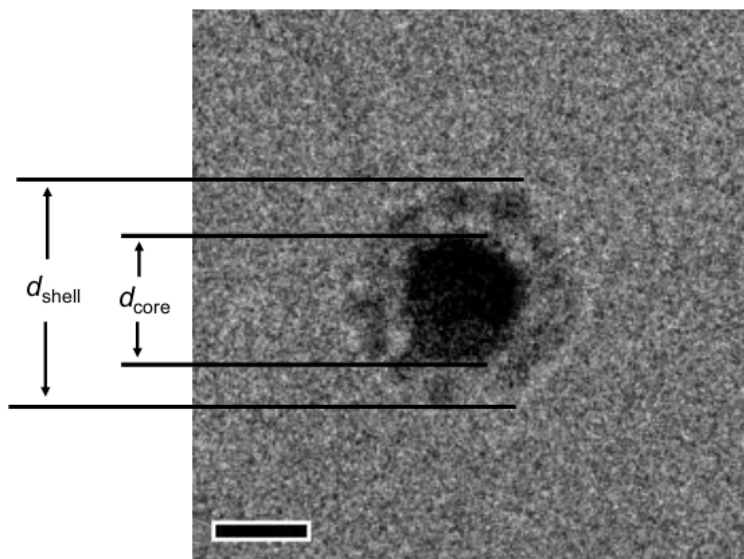


Figure S1. Method for measuring the monolayer width. The monolayer used in this example is comprised of the Finke-Droege ion (Zn(II) form). Bar = 5 nm.

The monolayer thickness is calculated as follows:

$$\text{thickness} = (d_{\text{shell}} - d_{\text{core}}) / 2 \quad (\text{S1})$$

Specific method. A method was devised to obtain accurate monolayer-thickness values for particles of variable size. For each of the three POM structures, the best images were chosen by considering the clarity and focus of the monolayers, and the minimum number of POMs in the background (a direct function of POM concentration). Moreover, from each set, the roundest particles (most nearly circular gold cores in the 2D images) were measured, so that only orientations on similarly-curved surfaces were examined. For each selected NP, the full diameter was measured, including the Au(0)-core and the POM monolayer (Figure S2, demonstrated using a 14-nm core particle).

Each diameter was measured while ensuring it was perpendicular to the monolayer on that specific curved area. To ensure this, the measurements were required to pass through the center of the NP, in orientations not complicated by obvious surface defects. Next, the Au(0)-core diameter was measured using a trace coincident with that used to measure the full diameter. The monolayer thickness was then determined by subtracting the core diameter from the full diameter, and dividing the result by two (eq S1).

In principle, the monolayer thickness should correspond in size to one of the POM dimensions, thus defining POM orientation. For instance, if the monolayer thickness is equal to the long dimension, the POMs are 'standing up' on the particle, and if it is equal to the small dimension, the POMs are 'lying down'. Each selected NP was measured twice using the method in Figure S2. For each POM-gold NP combination, multiple measurements were taken (see specific numbers for each in footnote in the text of the manuscript), and from those, an average and standard deviation were calculated for monolayers of each of the three structures.

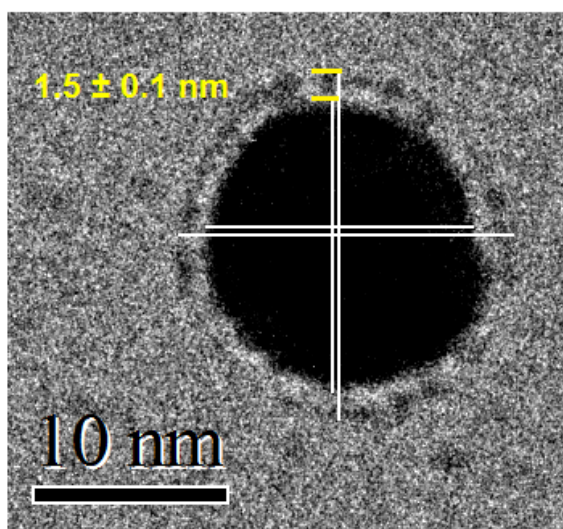


Figure S2. Cryo-TEM image of α -AlW₁₁O₃₉⁹⁻-protected Au(0) NP in vitreous (glassy) water showing the measuring method. The long white line represents the full diameter (including the Au(0)-core and the POM monolayer) and the short white line represents the Au(0)-core diameter. The difference between the two represents the thickness of the monolayer as shown in yellow.

2. Size distribution of the smaller (6.4 nm) Au NPs

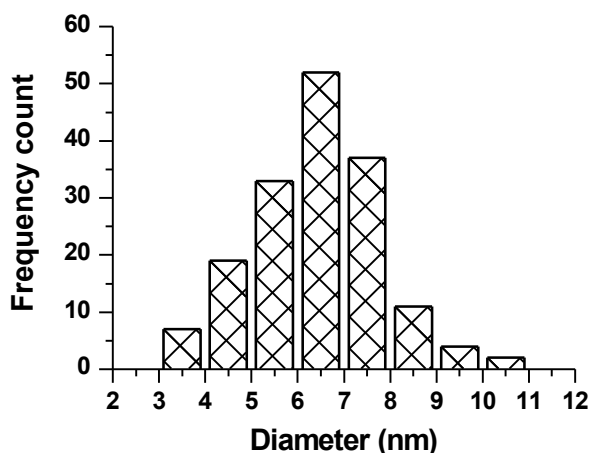


Figure S3. Size distribution of the citrate-stabilized Au NPs.

Based on counting ca. 160 NPs in TEM images, the average diameter is 6.4 nm with a standard deviation of 1.4 nm.

3. Electron density distribution in the Preyssler ion

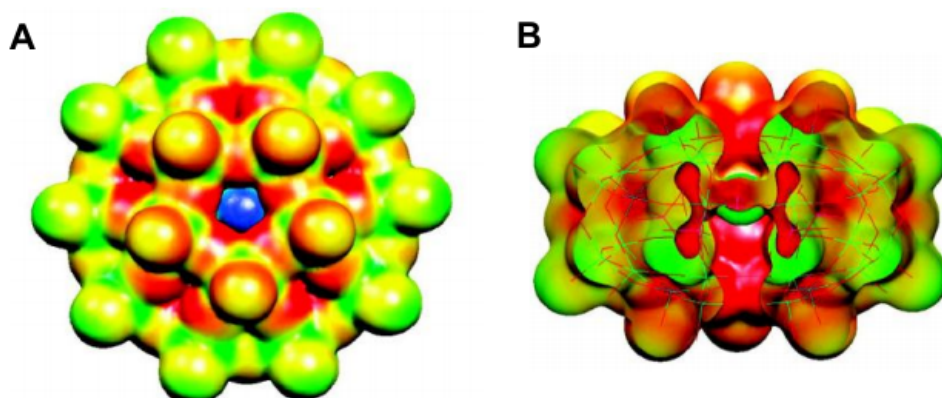


Figure S4. Top (A) and side (B, one-half of the molecule) views of the molecular electrostatic potential (MEP) distribution for $[\text{NaP}_5\text{W}_{30}\text{O}_{110}]^{14-}$.

The cavity is the most nucleophilic (B, red region), where the Na^+ is fully stabilized (blue in A). The faces (red with yellow for the terminal oxygen atoms, are significantly more nucleophilic than the “sides” of the structure, indicated by the cooler colors of yellow to green. Reprinted with permission from the American Chemical Society.¹⁰

4. Reference

1. J. J. Cowan, C. L. Hill, R. S. Reiner and I. A. Weinstock, in *Inorg. Synth.*, ed. D. Coucouvanis, John Wiley & Sons, Inc., New York, 2002, vol. 33, pp. 18-23.
2. J. J. Cowan, A. J. Bailey, R. A. Heintz, B. T. Do, K. I. Hardcastle, C. L. Hill and I. A. Weinstock, *Inorg. Chem.*, 2001, **40**, 6666-6675.

3. I. A. Weinstock, J. J. Cowan, E. M. G. Barbuzzi, H. D. Zeng and C. L. Hill, *J. Am. Chem. Soc.*, 1999, **121**, 4608-4617.
4. R. Contant, in *Inorg. Synth.*, ed. A. P. Ginsburg, John Wiley & Sons, New York, 1990, vol. 27, pp. 104-111.
5. R. G. Finke, M. W. Droege and P. J. Domaille, *Inorg. Chem.*, 1987, **26**, 3886-3896.
6. A. Neyman, L. Meshi, L. Zeiri and I. A. Weinstock, *J. Am. Chem. Soc.*, 2008, **130**, 16480-16481.
7. Y. Wang, A. Neyman, E. Arkhangelsky, V. Gitis, L. Meshi and I. A. Weinstock, *J. Am. Chem. Soc.*, 2009, **131**, 17412-17422.
8. Y. Wang, O. Zeiri, A. Neyman, F. Stellacci and I. A. Weinstock, *ACS Nano*, 2011, **6**, 629-640.
9. N. R. Jana, L. Gearheart and C. J. Murphy, *Langmuir*, 2001, **17**, 6782-6786.
10. J. A. Fernández, X. López, C. Bo, C. de Graaf, E. J. Baerends and J. M. Poblet, *J. Am. Chem. Soc.*, 2007, **129**, 12244-12253.